

Fig. 1S

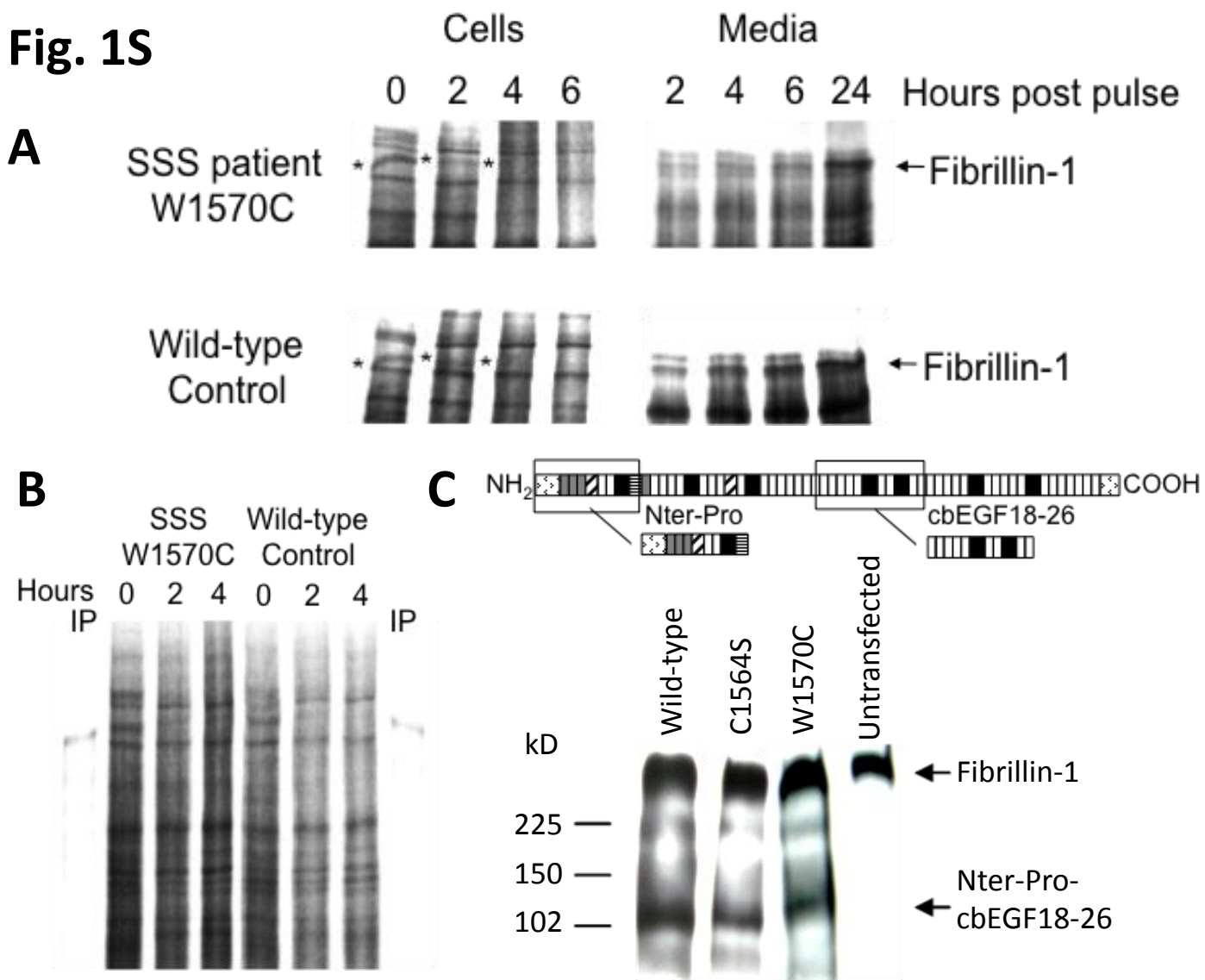
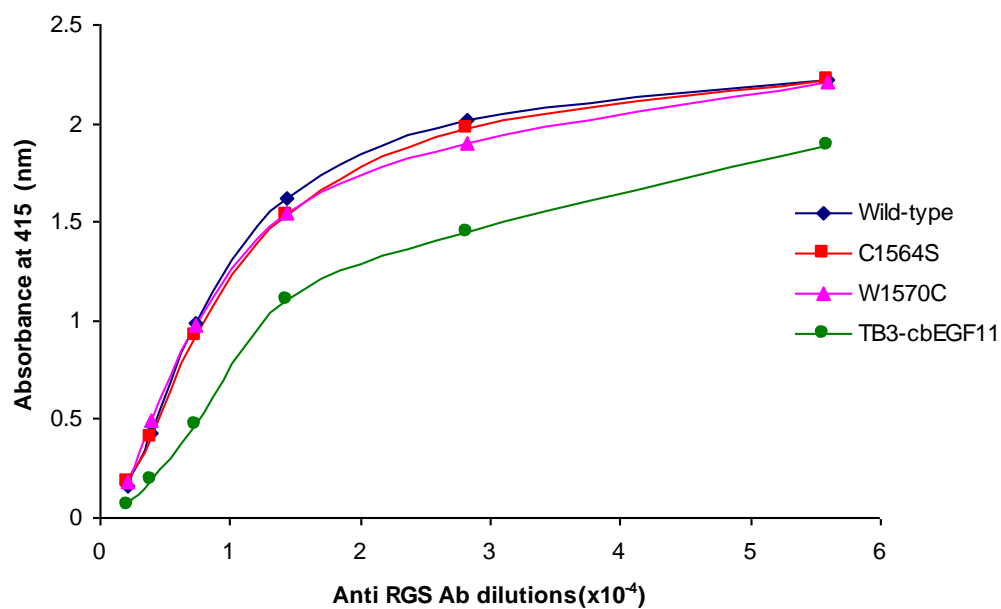


Figure 1S. Proper synthesis and trafficking of fibrillin-1 in SSS. A) Pulse-chase analyses of dermal fibroblasts from a SSS patient heterozygous for *FBN1* mutation W1570C and a control individual. Both samples show labelling of pro-fibrillin-1 (asterisks) at the end of the pulse (time point 0) that is gradually cleared from the cells; processed fibrillin-1 accumulates in the media (arrow) in both the patient and control samples. **B)** The identity of pro-fibrillin-1 in the cellular fraction was confirmed on a separate gel by comparison to the position of migration of immunoprecipitated pro-fibrillin-1 (IP). **C)** Western blot analysis of media derived from MSU-1.1 cells stably transfected with a construct encoding a recombinant peptide linking an N-terminal fragment of fibrillin-1 encompassing the proline rich domain (Nter-Pro) and a more C-terminal fragment spanning cbEGF-like domains 18-26 and encompassing TB4 (Nter-Pro-cbEGF18-26). All forms (wild-type, C1564S and W1570C) were secreted into the media. Endogenously-encoded fibrillin-1 is expressed in all cells, but recombinant protein is lacking in untransfected cells. An antibody recognizing an epitope in the proline-rich domain was used. Molecular weight markers are indicated.

Figure 2S

A



B

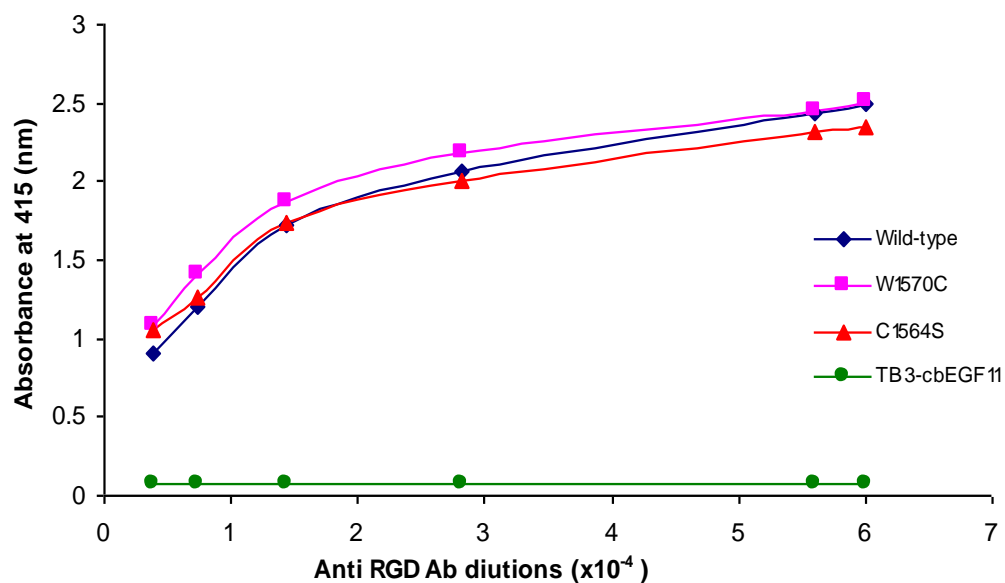


Figure 2S. ELISA analysis of cbEGF22-TB4-cbEGF23 recombinant fragments to an anti-RGD antibody. Each protein sample was plated at 5 μ M concentration and analyzed using doubling dilutions of the primary antibody (1:125 to 1:8,000). Each dilution was assayed in triplicate. **A)** Anti-RGS-His antibody was used to determine the amount of each His-tagged protein that bound to the plate. **B)** Anti-RGD antibody was used to determine the amount of RGD epitope that was exposed and available for binding. Both the W1570C and the C1564S fragments bind at least as well as the Wild-type fragment. A TB3-cbEGF11 fragment (which does not encode an RGD sequence) showed no binding to the anti-RGD antibody, as expected.

Figure 3S

A

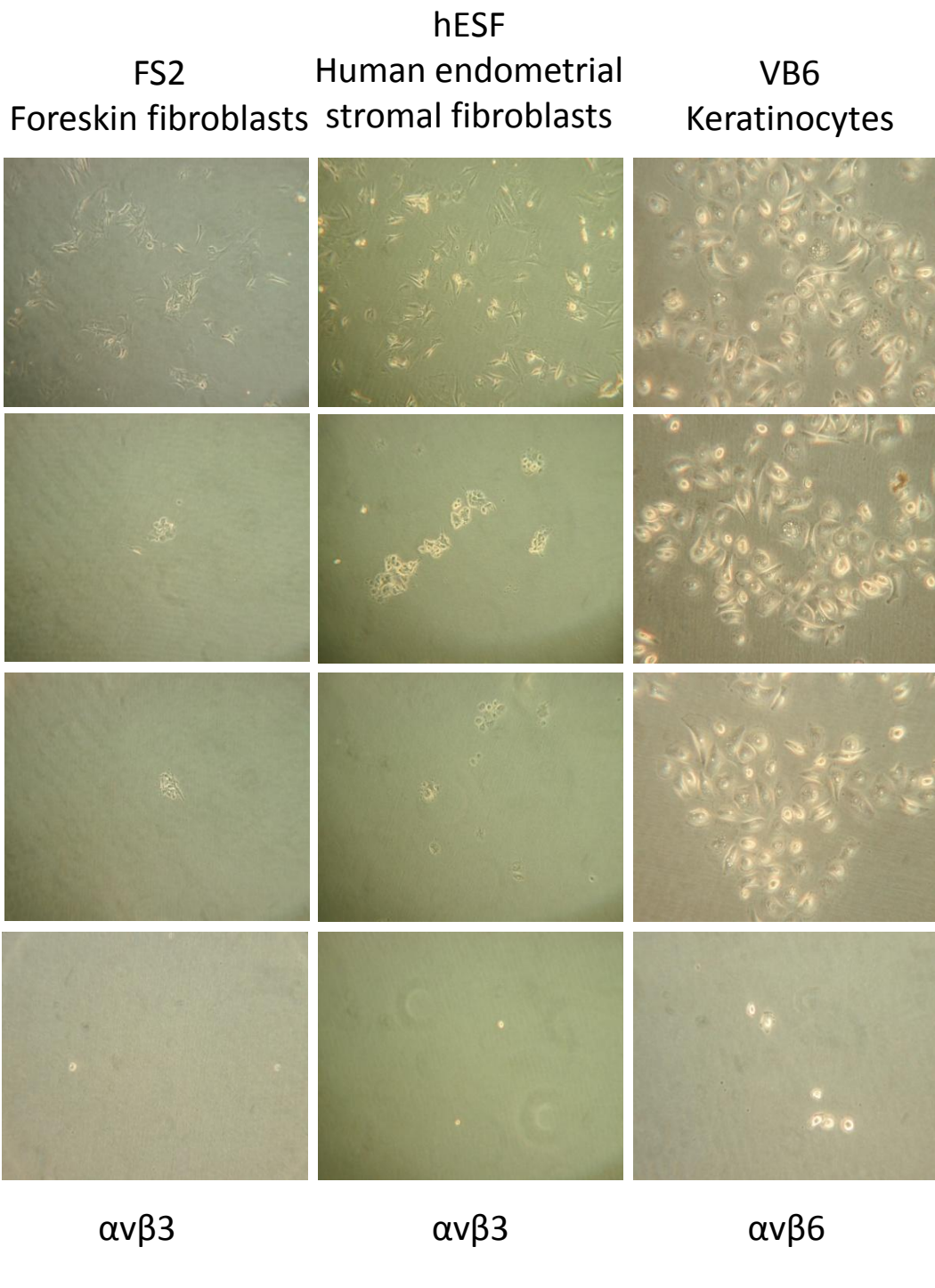


Figure 3S. A) Cell attachment and spreading assay. Equal numbers of the indicated cell types were added to plates coated with the indicated fibrillin-1 recombinant fragments (5 μ M) or bovine serum albumin (BSA) as a negative control. While cell spreading data were derived from the analysis of the morphology of 200 cells viewed by phase contrast microscopy (a representative panel of each cell type plated on to each construct is shown), the attachment data were quantified (Fig.3 in manuscript) by monitoring the uptake of crystal violet stain. Integrins known to form focal adhesions when bound to fibrillin fragments are indicated for each cell type.

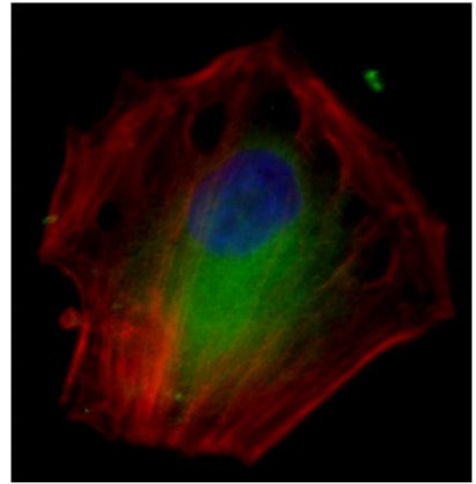
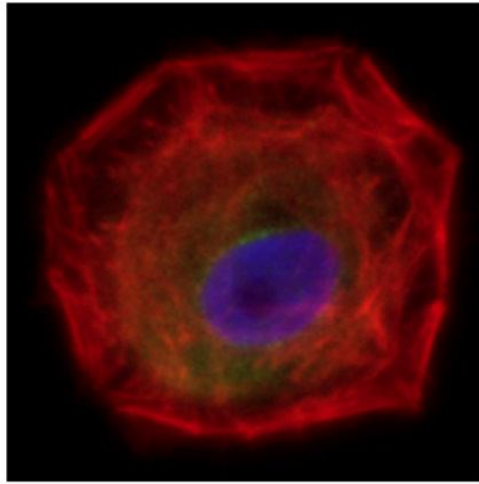
Figure 3S

B

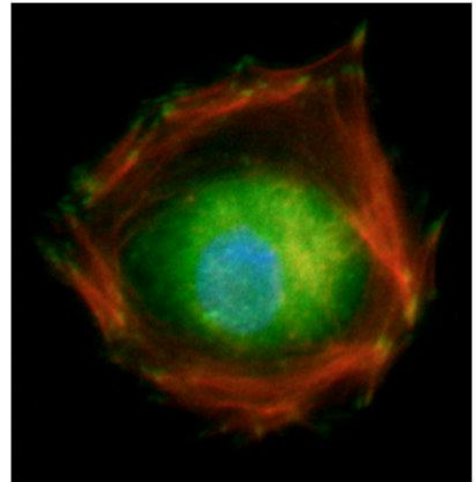
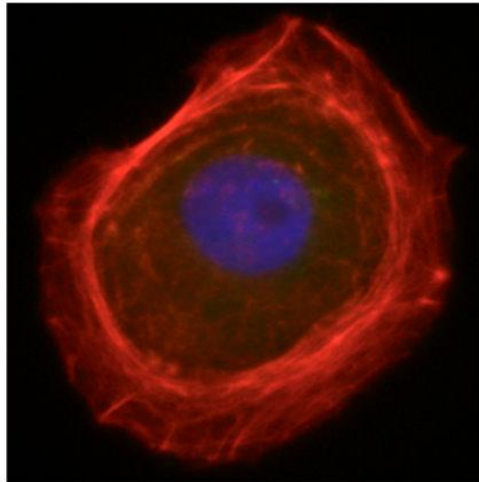
VB6

FS2

$\alpha5\beta1$ Ab



$\alpha v\beta3$ Ab



$\beta6$ Ab

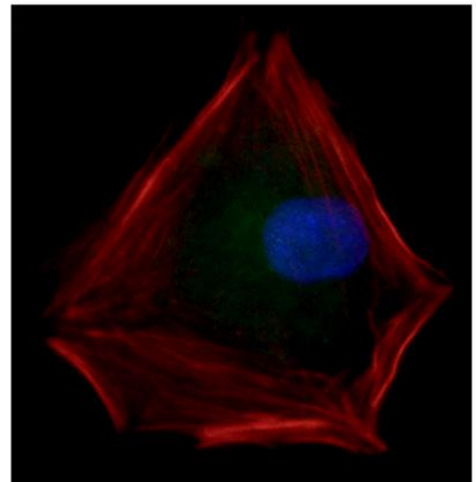
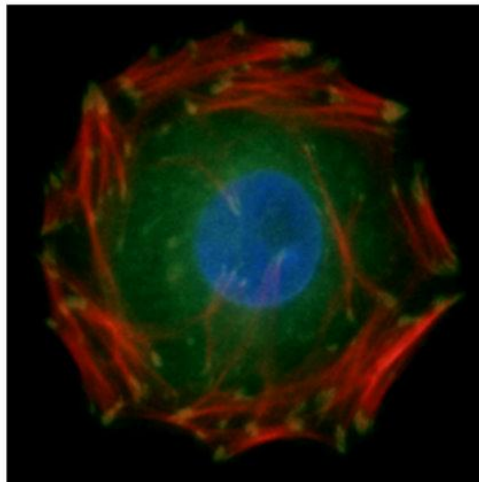


Fig 3S. B) Expression of integrins in VB6 and FS2 cells.

Immunocytochemistry using either VB6 or FS2 cells for the indicated integrin subtypes (green signal). Actin filaments are labeled with Phalloidin-Texas red (Invitrogen)(red signal). Nuclei are stained with DAPI (blue signal). VB6 cells show positive staining for $\beta6$ integrin, mainly in punctate foci marking focal adhesions at the cell surface. FS2 cells show expression of both $\alpha5\beta1$ and $\alpha v\beta3$ integrins, but only the latter localizes to focal adhesions.